



Cite this: *Biomater. Sci.*, 2023, **11**, 7856

## Fluorescent liposomal nanocarriers for targeted drug delivery in ischemic stroke therapy

Michael R. Arul,<sup>†a</sup> Ibtihal Alahmadi,<sup>†b</sup> Daylin Gamiotea Turro,<sup>d</sup> Aditya Ruikar,<sup>a,b</sup> Sama Abdulmalik,<sup>b</sup> Justin T. Williams,<sup>d</sup> Basavaraju G. Sanganahalli,<sup>e</sup> Bruce T. Liang,<sup>f</sup> Rajkumar Verma <sup>\*cd</sup> and Sangamesh G. Kumbar <sup>\*a,b,c</sup>

Ischemic stroke causes acute CNS injury and long-term disability, with limited treatment options such as surgical clot removal or clot-busting drugs. Neuroprotective therapies are needed to protect vulnerable brain regions. The purinergic receptor P2X4 is activated during stroke and exacerbates post-stroke damage. The chemical compound 5-(3-Bromophenyl)-1,3-dihydro-2H-Benzofuro[3,2-e]-1,4-diazepin-2-one (5BDBD) inhibits P2X4 and has shown neuroprotective effects in rodents. However, it is difficult to formulate for systemic delivery to the CNS. The current manuscript reports for the first time, the synthesis and characterization of 5BDBD PEGylated liposomal formulations and evaluates their feasibility to treat stroke in a preclinical mice model. A PEGylated liposomal formulation of 5BDBD was synthesized and characterized, with encapsulation efficacy of >80%, and release over 48 hours. *In vitro* and *in vivo* experiments with Nile red encapsulation showed cytocompatibility and CNS infiltration of nanocarriers. Administered 4 or 28 hours after stroke onset, the nanoformulation provided significant neuroprotection, reducing infarct volume by ~50% compared to controls. It outperformed orally-administered 5BDBD with a lower dose and shorter treatment duration, suggesting precise delivery by nanoformulation improves outcomes. The fluorescent nanoformulations may serve as a platform for delivering and tracking therapeutic agents for stroke treatment.

Received 2nd June 2023,  
Accepted 18th October 2023  
DOI: 10.1039/d3bm00951c  
rsc.li/biomaterials-science

## Introduction

Central Nervous System disorders, including Alzheimer's disease, Parkinson's disease, and Ischemic stroke, are increasingly prevalent worldwide.<sup>1,2</sup> While several drugs have been created to treat and manage these neurological disorders, drug delivery to the targeted site remains a significant obstacle.<sup>3</sup> To address drug delivery challenges and enhance medication's therapeutic effectiveness, various drug delivery systems such as polymeric microparticles, nanoparticles, and self-micro and nano-emulsifying drug delivery systems (SMEDD/SNEDD) have been developed.<sup>4-9</sup>

Liposomal nanocarriers have emerged as a potential drug delivery system for lipophilic drugs and are commonly prepared using non-toxic natural phospholipids or cholesterol.<sup>10</sup> To improve the *in vivo* stability and circulation time, polyethylene glycol (PEG) is often covalently linked to lipids in PEGylated liposomes.<sup>11</sup> The use of liposomal formulations not only improves the solubility of lipophilic drugs, but also enhances their pharmacokinetics and biodistribution due to the prolonged circulation time in the body.<sup>12-15</sup>

Ischemic stroke is a prevalent cause of disability in the United States, arising from a blockage in blood supply to the brain, usually caused by a clot that travels to the brain.<sup>16</sup> The occurrence of ischemic stroke results in the formation of infarcts, which are non-salvageable areas of dead tissue (known as the core region of stroke) within the brain parenchyma. The surrounding region of the core, known as the penumbra, contains vulnerable cells that can be rescued with appropriate neuroprotective therapy.<sup>17-19</sup> However, apart from clot-busting drugs and surgical clot removal, there are currently no approved therapies for stroke.<sup>20</sup>

We recently demonstrated that the purinergic receptor P2X4 (P2X4R) is activated following acute injuries like ischemic stroke, which can worsen post-stroke damage.<sup>21</sup> Inhibition of the P2X4R with a chemical compound such as 5-(3-

<sup>a</sup>Department of Orthopaedic Surgery, University of Connecticut Health, Farmington, CT, USA. E-mail: kumbar@uchc.edu; Fax: +1 (860) 679-1474; Tel: +1 (860) 679-3955<sup>b</sup>Department of Biomedical Engineering, University of Connecticut, Storrs, CT, USA<sup>c</sup>Department of Materials Science and Engineering, University of Connecticut, Storrs, CT, USA<sup>d</sup>Department of Neurosciences, UConn Health, Farmington, CT, USA.

E-mail: raverma@uchc.edu; Tel: +1(860)679-4552

<sup>e</sup>Department of Radiology and Biomedical Imaging, Yale University School of Medicine, New Haven, CT, USA<sup>f</sup>Calhuan Cardiology Centre, UConn Health, Farmington, CT, USA

† Equally contributed.



Bromophenyl)-1,3-dihydro-2*H*-Benzofuro[3,2-*e*]-1,4-diazepin-2-one (5BDBD) can reduce this damage and provide a neuroprotective and neurorehabilitative effect in a mouse model of ischemic stroke.<sup>22</sup> However, treatment of any central nervous system (CNS) disorder with a therapeutic agent, formulated or not, requires transport across the blood–brain barrier (BBB). During the acute phase of ischemic stroke, the BBB is compromised, which presents a natural advantage for drug delivery to the site of brain injury.<sup>23</sup>

In our previous study, we demonstrated the neuroprotective effects of orally administered 5-BDBD (1 mg per kg per day × 3 days) in a mouse model of ischemic stroke. However, due to its insolubility in physiological solvents, the drug was given as an oral suspension, which is not a viable option for stroke patients who rely mostly on parenteral drug administration during the acute phase of stroke injury.<sup>21</sup> Therefore, there is a need to explore alternative drug delivery options for clinics.<sup>24</sup> Here, we present the synthesis and characterization of a PEGylated liposomal formulation of 5BDBD and evaluate its feasibility to treat stroke in a preclinical mouse model. To visualize liposomal uptake by cells *in vitro* and track them *in vivo*, we encapsulated Nile red (NR) fluorescent dye in the liposomes. We characterized the liposomes for particle size, shape, drug encapsulation, and *in vitro* release kinetics. Furthermore, we assessed liposomal uptake and toxicity by culturing them with human skin fibroblasts *in vitro* and selective accumulation in the ischemic brain tissue in mice after stroke following tail vein injection. This is the first report of a liposomal formulation of 5BDBD, and our results suggest that it could be a promising drug delivery system for the treatment of stroke.

## Results and discussion

### Formulation of liposome nanoparticles (LNP)

The lipid nanoparticle (LNP) system offers flexible drug delivery properties, including control over size, particle size distribution,

matrix hydrophobicity/hydrophilicity, and surface charge, using FDA-approved excipients that can cross the blood–brain barrier for stroke applications.<sup>24</sup> In this study, we developed pegylated LNPs containing 5BDBD and Nile Red dye as injectables that can accumulate in stroke areas through the disrupted BBB, thereby enhancing the drug's therapeutic effectiveness. Fig. 1 illustrates the formulation of liposome nanoparticles containing drug and dye, and the preparation concentrations of each group are summarized in Table 1. We used DPPC, DOPC, DPPG, and DSPE-PEG2000 amine phospholipids based on their history as biocompatible carrier systems and their FDA-approval status in drug delivery systems.<sup>25–28</sup> The LNPs were prepared by film formation and hydration, a straightforward and elegant process.<sup>29–31</sup> Further dispersion of the lipid layer in a suitable solvent and extrusion through a polycarbonate membrane allowed to produce homogeneously sized liposomal nanoparticles.<sup>32</sup> Liposomes prepared using thin-film hydration method are quite common for delivery of hydrophobic drugs and are being used for delivery drugs to the brain in conditions like stroke. Utilization of liposomal drug delivery system made by thin-film hydration method has been reported recently for delivery of drugs like edaravone, NMITL118RT+ and ligustrazine for treatment of stroke which signifies that the method used by the authors is a reliable for preparation and delivery of chemical moieties to brain in stroke condition.<sup>33–35</sup> Liposome formulations made by thin-film hydration method has also been used for delivery of imaging agents for MRI imaging, although no combination of drug and dye loaded delivery system has yet been reported.<sup>36,37</sup> Hence, here we successfully report the liposome nanoparticle formulation containing a combination of both drug (5-BDBD) + dye (Nile Red) for drug delivery as well as imaging which will eliminate the need for usage of two separate systems for delivery and imaging and make the drug delivery and imaging more efficient in patients with stroke.

The addition of PEG to liposomal drug delivery systems is known to increase their stability and prolong their circulation time, allowing for passive targeting in leaky vasculature.<sup>38,39</sup>

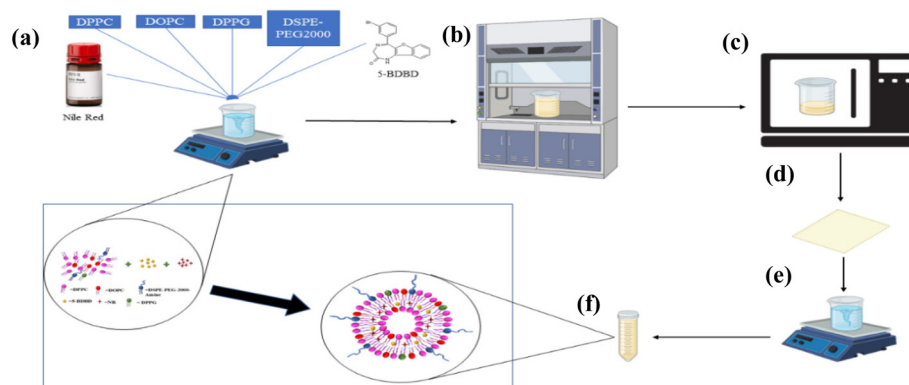


**Fig. 1** Schematic diagram for the preparation of 5BDBD encapsulated liposomes by freeze–thaw cycles. The process is as follows: (a) mixing of ingredients in solvent with drug and dye, (b) evaporation of solvent in  $N_2$  atmosphere, (c) overnight incubation in vacuum oven, (d) formation of thin film, (e) redispersion and temperature cycling and (f) final formulation. The drug 5BDBD and Nile Red dye is incorporated in the bilayer of the PEGylated liposome due to its hydrophobic nature. The freeze–thaw approach enhances drug encapsulation efficiency, while the inclusion of Nile Red dye allows for tracking and visualization of the liposomes in biological systems.



**Table 1** Formulation ratios of different components used in formulation of LNPs

Lipid nanoparticles	Dye (mole ratio)	DPPC (moles%)	DOPC (moles%)	DPPG (moles%)	PEG-2000-AMINE (moles%)	5BDBD (mole ratio)
Lipo		47	47	0.5	5.5	
Lipo + dye	1 : 500	47	47	0.5	5.5	
Lipo + 5BDBD		47	47	0.5	5.5	1 : 100
Lipo + 5BDBD + dye	1 : 500	47	47	0.5	5.5	1 : 100

Surface modification of nanocarriers with PEG or methylated PEG is a widely used technique to avoid opsonization and increase circulation time.<sup>40</sup> In this study, liposomal formulations were designed with a PEG-amine (DSPE-PEG200) to enable both passive stroke targeting and stabilization. Previous studies have used liposomes containing *N*-oleoyl ethanolamine phosphatidylcholine complex with DSPE-PEG for stroke treatment.<sup>41,42</sup> However, 5BDBD liposomal formulations with PEG-amine have not been reported for stroke applications. The reported PEG surface-modified liposomes in this study support their stability, long circulation time, and passive targeting in stroke.

### Particle size analysis and surface morphology

The shape, size, and morphology of particles are crucial for injectable drug delivery systems and their *in vivo* performance. In normal conditions, a size range of 100 nm is effective in crossing the BBB, but in conditions like stroke with increased

permeability, the particle size range for crossing the BBB increases.<sup>43,44</sup> Larger particles with irregular shapes can cause non-predictable drug release profiles and may block blood vessels.<sup>45,46</sup> Reported liposomal nanocarriers are spherical with a narrow size distribution that ranges from 50–80 nm, depending on the type. The empty lipid nanocarriers have a size of 50 nm, while drug-loaded ones have a size of 60 nm. The drug-loaded liposomes have a size of 70 nm, while the dye-loaded ones are smaller at 50 nm. Fig. 2(a) shows a typical particle size histogram obtained from light scattering experiments, demonstrating the variation in particle size based on its makeup. The overall particle size of all formulations ranges between 40–60 nm, which is smaller than what was reported previously.<sup>41,47,48</sup> The drug + dye-encapsulated nanocarriers have the smallest median particle size of 60 nm compared to other formulations. The changes in particle size of the nanocarriers may be due to the interaction between the encapsulated materials and the lipid in

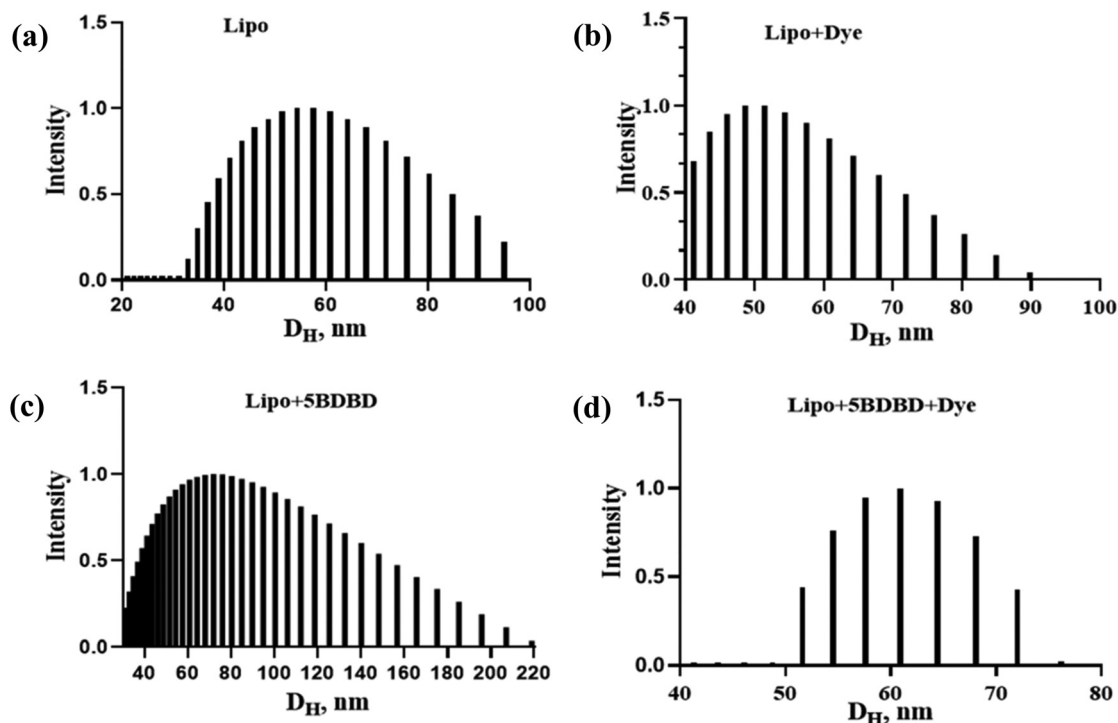


**Fig. 2** The particle size distribution of different liposome formulations, as determined by dynamic light scattering. (a) The lipid only (Lipo) and (b) lipid + dye (lipo + dye) formulations exhibit smaller particle sizes compared to (c) lipid + drug (lipo + 5BDBD) and (d) lipid + dye + drug (lipo + 5BDBD + dye). The larger sizes observed in the latter two formulations suggest successful encapsulation of hydrophobic drug molecules within the liposome nanoparticles. This finding highlights the potential of these injectable drug-loaded liposomes for targeted drug delivery.



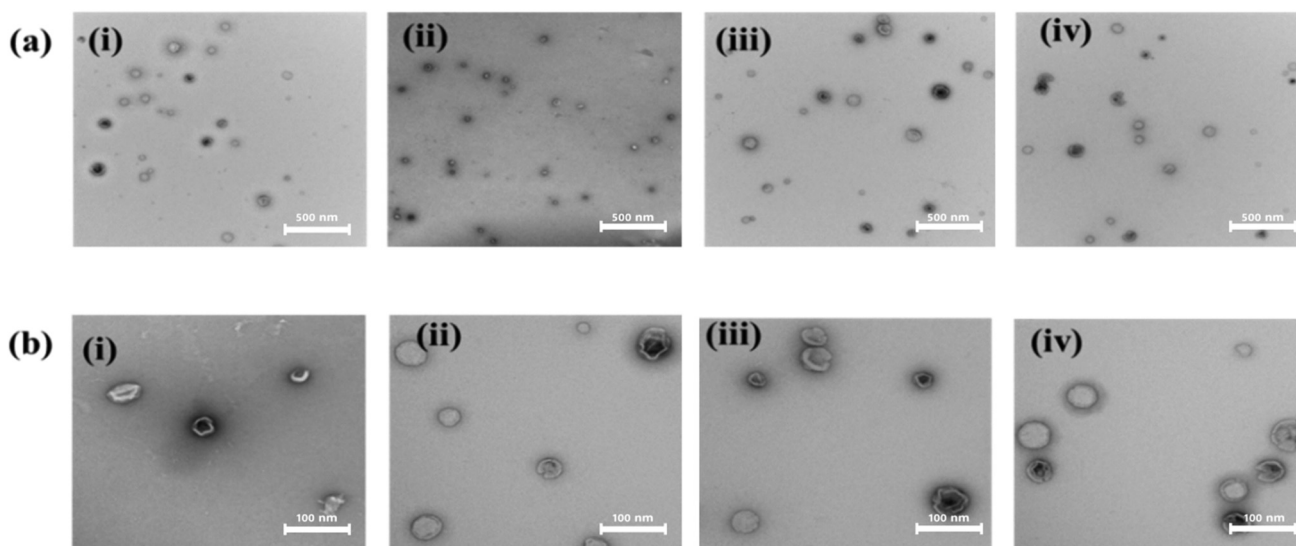


**Fig. 3** TEM images at two different magnifications of (a) 500 nm (scale bar) and (b) 100 nm (scale bar) where (i) lipid only; (ii) lipid + drug; (iii) lipid + dye; (iv) lipid + drug + dye. TEM analysis confirms formation of spherical liposomes for all formulations, exhibiting unilamellar morphology and smooth surface.

minimizing energy and stability.<sup>49</sup> The liposomal formulations are spherical and unilamellar, with a smooth surface morphology, as shown in TEM images in Fig. 3(a) and (b). Such nanocarriers are ideal as injectables, as demonstrated in previous literature.<sup>50–53</sup>

#### Drug encapsulation efficiency

The encapsulation efficiency of Lipo + 5BDBD and Lipo + 5BDBD + Dye was determined to be 85.74% and 83.38% respectively, as shown in Fig. 4. High encapsulation efficiency is advantageous in reducing drug waste during formulation

development and requiring less formulation for dosing.<sup>54</sup> The one-pot synthetic protocol employed in this study resulted in the highest EE when compared to other nanocarriers reported in the literature.<sup>55–57</sup> Moreover, the addition of dye in the formulation led to a slower drug release rate, possibly due to interactions between the dye and the drug which may have caused slower diffusion of drug through the carrier, as demonstrated in Fig. 4.<sup>58</sup> This may be disadvantage but at the same it also enabling direct visualization of liposome formulation. Therefore, slight slower rate of 5-BDBD release with addition of dye still show advantage.

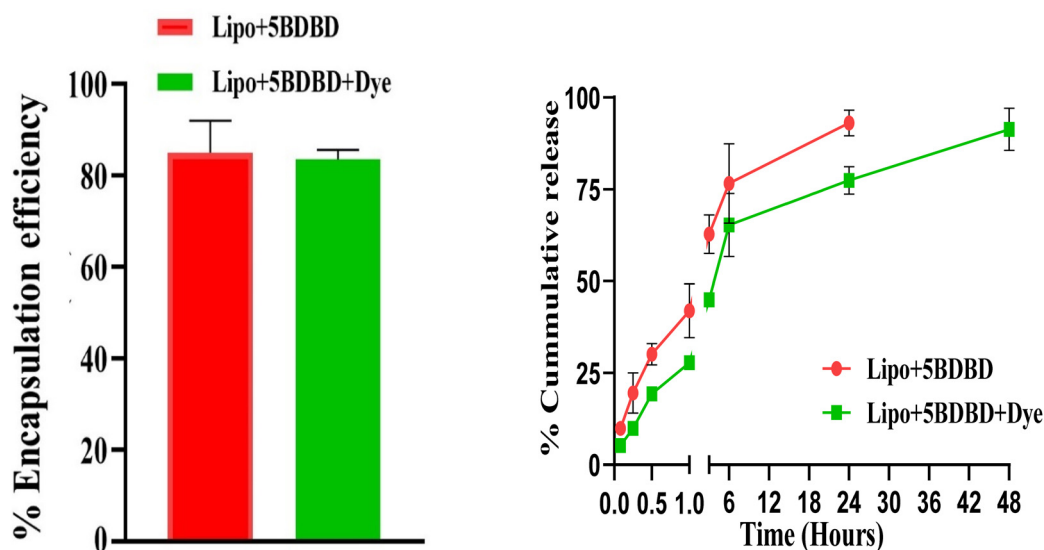


**Fig. 4** % Encapsulation efficiency (left) and % cumulative release (right). both lipo + 5BDBD and lipo + 5BDBD + dye exhibited excellent encapsulation efficiency, around 80%. The addition of dye resulted in prolonged drug release, up to 48 hours. This suggests potential applications in controlled drug delivery.





### ***In vitro* drug release and kinetics**

The *in vitro* drug release study revealed that 95.4% of 5BDBD was released within 24 hours from the formulation containing only the drug (Fig. 4). However, in the formulation containing both the drug and NR dye, 87.3% of the drug was released within 24 hours, and the release continued up to 48 hours (Fig. 4). The presence of dye in the formulation resulted in a slower drug release rate, which could be attributed to the complex drug–dye interaction.<sup>1</sup> Similar systems have been reported in the literature, where the presence of an additive in the formulation reduced the rate of drug release.<sup>59,60</sup>

The diffusion coefficients were calculated using eqn (1) and (2). Both drug-alone and drug + dye formulations exhibited diffusion coefficients greater than 0.5, indicative of anomalous and non-Fickian drug release mechanisms.<sup>61</sup> In such formulations, the drug release is regulated by both diffusion and swelling.<sup>62,63</sup> Liposomal formulations containing a lipophilic drug, such as 5BDBD, have also shown similar release behaviour.<sup>64</sup>

### ***In vitro* cellular uptake and toxicity**

The cytotoxicity of the nanocarriers and their uptake by cells were evaluated using human skin fibroblasts in accordance with ISO standards.<sup>65</sup> The results showed that the fibroblasts efficiently internalized the nanocarriers, and the fluorescence intensity within the cells increased with time (Fig. 5(a)). The metabolic activity of the fibroblasts was assessed using the MTS assay over 72 hours under different treatment conditions (Fig. 5(b)). The results revealed that the nanocarriers did not affect the metabolic activity of the fibroblasts at 3, 24, and 72 hours, indicating their cytocompatibility. Previous studies using similar lipids and drugs have also shown compatibility with fibroblasts and other tissue-specific cells.<sup>66–69</sup> The non-toxicity of the formulations containing 5 µg of 5BDBD may be attributed to the gradual and controlled release of the drug, thereby reducing cytotoxicity.

### **Visualization of liposomal nano formulations in the brain parenchyma after stroke**

Fig. 6 illustrates the distribution of dye-loaded liposomal nano formulations with and without the drug in the brain parenchyma of mice 3 days after stroke onset. The formulations, containing 1 mg per kg b.w equivalent of 5-BDBD, were administered *via* tail vein injection at 4 and 28 hours after stroke onset. The fixed brain sections of the 5BDBD treatment group revealed enhanced accumulation of 5BDBD LNPs in the perilesional cortex of the stroke brain, as shown in Fig. 6. This indicates that the nanocarriers accumulated in the perilesional cortex due to increased blood–brain barrier rupture, thus providing sustained neuroprotection.<sup>70</sup>

### **5BDBD NP provides uniform neuroprotection**

Our previous study on stroke treatment utilized 5BDBD treatment *via* oral administration (1 mg per kg b.w × daily for 3 days), which provided acute neuroprotection at 3 days after

stroke.<sup>22</sup> However, 5BDBD is insoluble in aqueous solvents, and the oral route is not practical for stroke patients as they often experience acute dysphagia during the acute stage of stroke.<sup>71</sup> Therefore, we developed pegylated liposomal nanocarriers to parenterally administer 5BDBD [Fig. 6 and 7]. Consistent with our earlier findings, liposomal 5BDBD formulations provide acute neuroprotective effects as compared to control LNPs.<sup>22</sup> Interestingly, we achieved similar significant neuroprotection (~50% reduction in infarct volume *vs.* control) with only two doses (4 and 28 hours after stroke onset) of 5BDBD nano formulation injection as compared to oral administration as previously published by us.<sup>22</sup> We further observed that 5BDBD liposome were present in brain parenchyma (Fig. 7). This data suggests that liposome formulation cross BBB to reach site of action. It is to be noted that during acute stroke condition BBB is compromised and become more permeable. This fact is very well established in the literature<sup>72–74</sup> and we also have previously published that drug loaded nanoparticle can penetrate BBB after stroke.<sup>75,76</sup> In fact, both of our *in vivo* data of neuroprotection (Fig. 6) and immunofluorescence data (Fig. 6) supports BBB permeability of our 5BDBD liposome formulation. These results suggest that precise delivery by nano formulation may provide better outcomes after stroke, even with a lower frequency of 5BDBD administration. As current standard of care relies only a clot buster drug tissue plasminogen activator (t-PA) and mechanical clot removal novel neuroprotective drug such as 5BDBD may be potential novel treatment for neuroprotective effects after stroke.

## **Experimental**

### **Materials**

1,2-dipalmitoyl-*sn*-glycerol-3-phosphocholine (16:0PC, DPPC), 1,2-dipalmitoyl-*sn*-glycerol-3-phospho-(1'-rac-glycerol) (16:0PG, DPPG), 1,2-dioleoyl-*sn*-glycerol-3 phosphocholine (di-6:0, DOPC), and DSPE-PEG 2000 Amine were purchased from Avanti Polar Lipids (Alabaster, AL) and used without further purification. Nile Red (NR) was purchased from NCI chemicals. 5-(3-Bromophenyl)-1,3-dihydro-2H-Benzofuro[3,2-*e*]-1,4-diazepin-2-one(5BDBD) obtained from Sigma Aldrich USA. Human Dermal Fibroblasts, adult (HDFa) (Cascade Biologics™), cell culture media DMEM, fetal bovine serum (FBS), phosphate-buffered saline (PBS), and DAPI were purchased from Fisher Scientific (Fair Lawn, NJ, USA). CellTiter 96® Aqueous One Solution Cell Proliferation Assay (MTS) was obtained from Promega (Madison, WI, USA). Ultrapure pure water (Millipore) and HPLC-grade solvents were used without further purification.

### **Formulation of liposome nanoparticles (LNP)**

To prepare the liposome nanoparticles, we utilized the thin film hydration method.<sup>32</sup> A chloroform mixture of DPPC/DOPC/DPPG/DSPE-PEG2000 amine in a molar ratio of 47/47/0.05/5 was homogenized. After evaporation of most of the



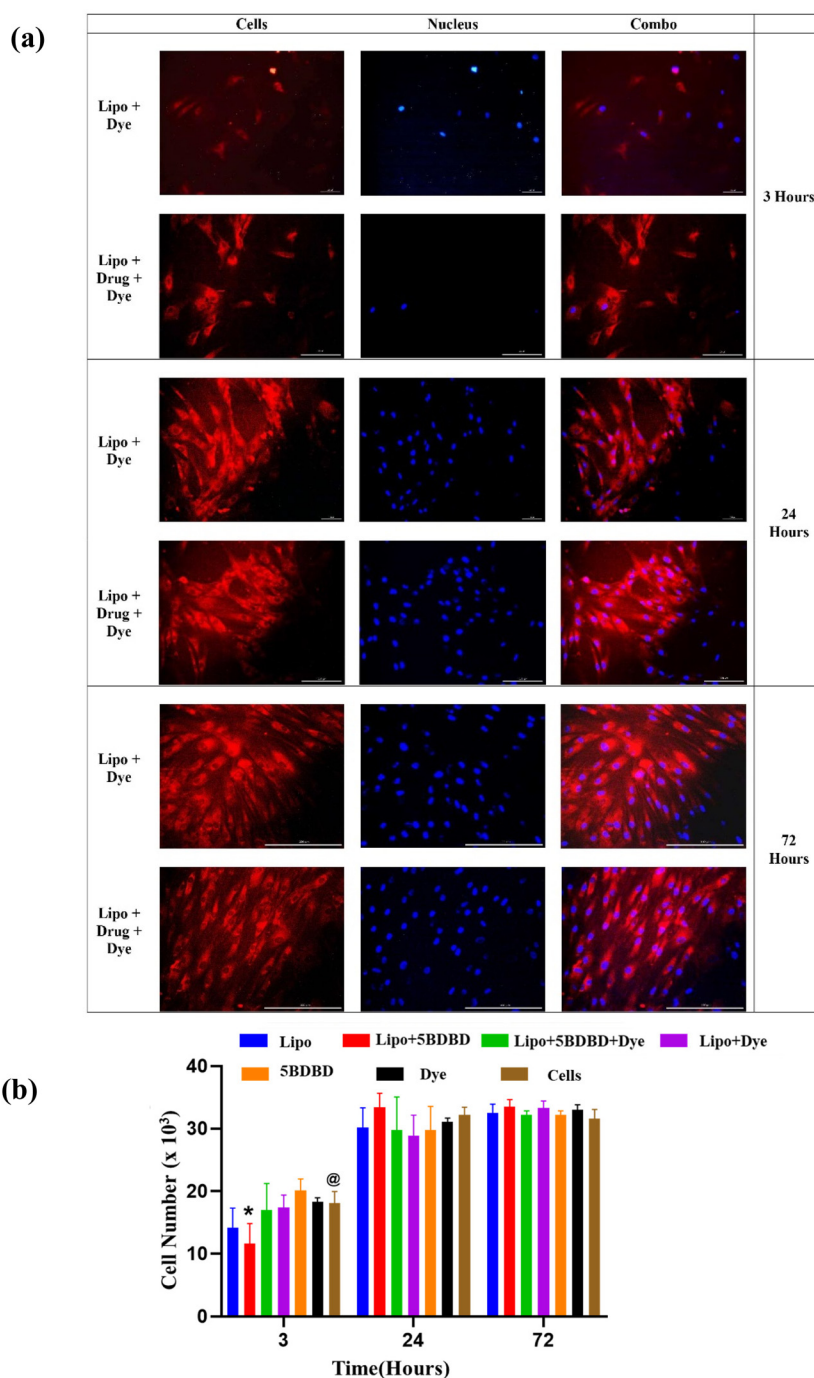


**Fig. 5** (a) Live–dead assay (scale: 100  $\mu\text{m}$ ). Fibroblasts maintained their morphology, with no apparent cell death observed upon the addition of nanoparticles. By day 3, both formulations exhibited an increase in live cell count. (b) Graphical representation of MTS Assay. Increased cell number is evident in all the cases, wherein formulation containing only drug displayed significant increase in cell count after 24 hours and maintained it through 72 hours. The live–dead and MTS assays demonstrated the biocompatibility and cell proliferation potential of both formulations. Two-way ANOVA with Tukey's multiple comparisons @ =  $p < 0.001$  vs. respective control, and \* =  $p < 0.0001$  vs. respective control  $n = 5$ .

solvent in a nitrogen atmosphere, the mixture was incubated in a vacuum oven overnight to remove any remaining solvent and form a thin film. In the first step of the preparation of drug and dye liposome nanoparticles, the drug (5BDBD) and dye (NR) were mixed with the lipids in a ratio of 1 : 100 (drug : lipid) and 1 : 500 (dye : lipid), respectively. The thin film was

then redispersed in deionized water to prepare a stock solution. After five cycles of vortexing and temperature cycling between 25  $^{\circ}\text{C}$  and 70  $^{\circ}\text{C}$ , the solution was extruded through a 100 nm membrane to obtain the desired size liposomes (<100 nm). Before *in vitro* and *in vivo* studies, the liposomes were diluted to the desired concentration with DI water or PBS.



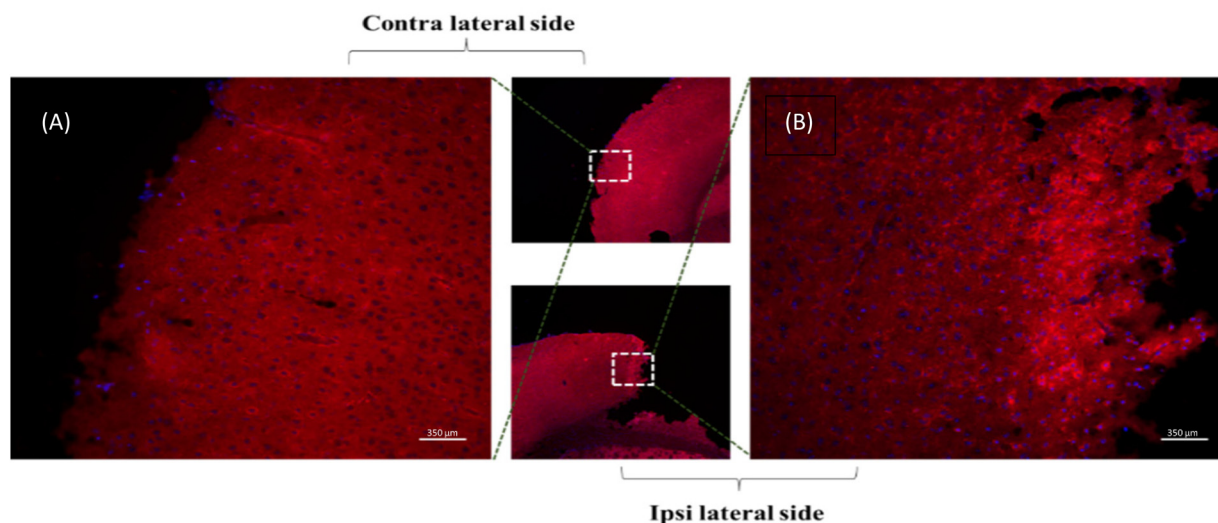


**Fig. 6** *In vivo* biodistribution lipo + 5-BDBD + dye in contralateral cortex (A) and ipsilateral perilesional cortex (B) of mice brain after stroke. *In vivo*, 5-BDBD-loaded liposome NPs show increased accumulation in the perilesional cortex of the ipsilateral hemisphere after stroke, utilizing the BBB rupture for targeted drug delivery to the ischemic brain tissue. This may hold promise for potential therapeutic applications in stroke treatment.

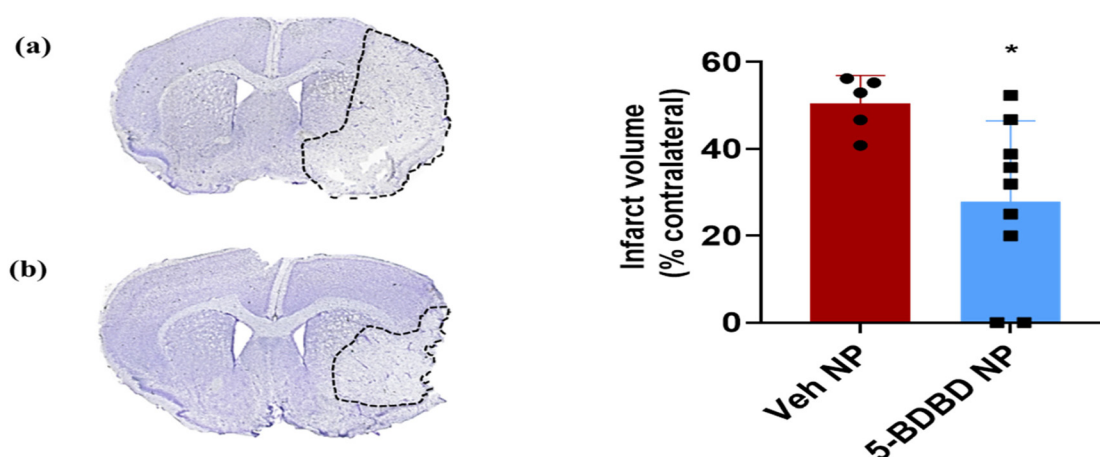


**Fig. 7** Representative cresyl violet stained section showing an infarct area (dotted line) in control (a) and 5-BDBD treatment group (b). Two-day treatment with lipo + 5BDBD + Dye (1 mg per kg I.V. per day in PBS) significantly ( $*p < 0.05$ ; vs. Veh NP unpaired *t*-test;  $n = 5-9$ ) reduced total hemispheric infarct volume in after 3 days of stroke. The lipo + 5BDBD + dye treatment effectively reduces the infarct volume after stroke, suggesting its potential as a therapeutic intervention for stroke management.

To distinguish between formulations, we used the following abbreviations:

1. Lipo – Liposome nanoparticle without any drug or dye.
2. Lipo + Dye – Liposome nanoparticle containing Nile red.
3. Lipo + Drug – Liposome nanoparticle containing 5BDBD.
4. Lipo + Drug + Dye – Liposome nanoparticle containing both 5BDBD and Nile red.

#### Particle size analysis

To determine the particle size of the liposome nanoparticles, dynamic light scattering method was used.<sup>77</sup> In this method, 0.1 wt% of the nanoparticle solution was dispersed in ultra-filtered DI water at 25 °C and subjected to a laser beam with a

wavelength of 632.6 nm. The scattering pattern of each formulation was then recorded to measure the particle size.

#### Surface morphology

To determine the surface morphology of the liposomes, Transmission Electron Microscopy (TEM) with negative staining was employed.<sup>78</sup> A 0.001 wt% aqueous formulation was placed on a 400 mesh Formvar/carbon film copper grid in a 5 μL droplet. Uranyl acetate at a concentration of 10 mg mL<sup>-1</sup> was used to stain the grid. After removing the excess solution and stain, the grid was dried and TEM imaging was performed at 80 kV to obtain images at scales of 500 nm and 100 nm, respectively.





### Drug encapsulation efficiency

To determine the encapsulation efficiency, 100  $\mu\text{L}$  of drug-containing formulations were evaporated on a heat stage, and the resulting dried samples were dispersed in 5 mL of ethanol and sonicated for 10 minutes using a probe sonicator. The drug content analysis was performed by subjecting the supernatant to UV spectrophotometry at 301 nm. The observed absorbance was converted to concentration using the standard curve. The encapsulation efficiency was calculated using eqn (1).<sup>79</sup> Each formulation was tested in triplicate and reported as Avg  $\pm$  Std. Dev.

$$\% \text{ EE} = \frac{\text{Actual Drug Conc.}}{\text{Drug Concentration used in formulation}} \times 100 \quad (1)$$

### *In vitro* drug release and kinetics

The *in vitro* drug release profiles of formulations containing 5-BDBD were evaluated in PBS with 20% ethanol at 37  $^{\circ}\text{C}$  under gentle agitation using an orbital shaker. Approximately 400  $\mu\text{g}$  of each formulation in 1 mL PBS were loaded into dialysis bags (MWCO 12 000 Da) and incubated in 6 mL of PBS with 20% ethanol to maintain a sink condition.<sup>80,81</sup> At pre-determined time intervals, 0.5 mL of the release medium was withdrawn and replaced with fresh PBS. The collected samples were analysed using a UV-Vis spectrophotometer at 301 nm to quantify the amount of 5-BDBD released.

The release kinetics of the drug were calculated using the Higuchi and Korsmeyer-Peppas models.<sup>62,63</sup> Each formulation was tested in triplicate and the results are presented as the average  $\pm$  standard deviation.

-Higuchi model equation:

$$\frac{M_t}{M_0} = Kt^{1/2} \quad (2)$$

-Korsmeyer-Peppas model equation:

$$\frac{M_t}{M_{\infty}} = kt^n \quad (3)$$

### *In vitro* cellular uptake

The *in vitro* cellular uptake of the formulations was assessed using human dermal fibroblast cells.<sup>77</sup> The cells were seeded at a density of approximately 5000 cells per well in a 48-well plate containing DMEM media. Subsequently, 200  $\mu\text{L}$  of cell culture media containing 5  $\mu\text{g}$  of 5BDBD was added to each well. After 72 hours of incubation, the wells were imaged at 20X magnification using a Nikon Eclipse E600 fluorescence microscope. The Texas red channel was employed to visualize Lipo + Dye, while the DAPI channel was used to visualize the nucleus of the cells. For each formulation, a sample size of  $n = 3$  was utilized, and the results were reported as the Avg  $\pm$  Std. Dev.

### Cytotoxicity and cell proliferation

To assess the cytotoxicity of 5BDBD and dye formulations, the metabolic activity of cultured fibroblasts was measured using

an MTS assay.<sup>82</sup> Human dermal fibroblasts were seeded at a density of  $\sim 5000$  per well in a 48-well plate supplemented with DMEM media. A 200  $\mu\text{L}$  of the cell culture media containing 5  $\mu\text{g}$  of 5BDBD was added to each well. Metabolic activity of the cells was measured at 3 h, 24 h, and 72 h by adding 40  $\mu\text{L}$  per well of MTS reagent at 37  $^{\circ}\text{C}$  for 1 h. The reaction was quenched by adding 50  $\mu\text{L}$  per well surfactant, and the absorbance of the media was measured at 490 nm. A sample size of  $n = 3$  was used per formulation, and results were reported as the Avg  $\pm$  Std. Dev.

### Injection of 5BDBD/Dye LNPs in a mice stroke model

All animal procedures were performed in accordance with the Guidelines for Care and Use of Laboratory Animals of School of Medicine, UConn Health Farmington CT and approved by Institutional Animal Care and Use Committee (IACUC) with Public Health Service (PHS) assurance number - A3471-01 (D16-00295). A total of 15 mice were randomly assigned to two groups: treatment with 5BDBD nanoparticles (Lipo + 5BDBD + Dye) or vehicle nanoparticles (Lipo only) 60 minutes after stroke. Nine mice received liposomal formulations containing 1 mg per kg b.w equivalent of 5BDBD, while six mice received liposomal nanocarriers. One mouse was excluded from the results due to death (one in the vehicle nano group) or technical failure (no observable infarct in the 5BDBD nano group). The accumulation of nanocarriers was visualized using NR dye, and treatment efficacy was assessed by measuring infarct volume.<sup>83</sup> Tail vein injections of liposomal formulations were administered twice after 4- and 28-hours following stroke onset. All mice were euthanized three days after the stroke.

### Stroke induction

The induction of stroke was performed by transiently occluding the Middle Cerebral Artery (MCA) for 60 minutes, followed by reperfusion for 3 days under isoflurane anaesthesia, as previously described.<sup>21,84</sup> The procedure involved a midline ventral neck incision and unilateral right MCA occlusion using a 6.0 silicone rubber-coated monofilament (size 602145/602245; Doccol Corporation, Sharon, MA), placed 10–11 mm from the bifurcation point of the internal carotid artery through an external carotid artery stump. During the procedure, rectal temperature was monitored and maintained at  $37 \pm 0.5$   $^{\circ}\text{C}$  with the aid of a heating pad. Cerebral blood flow was measured using a laser Doppler flowmeter (DRT 4/Moor Instruments Ltd, Devon UK) to confirm occlusion and reperfusion. Post-surgery, all animals were fed wet mash and given injectable normal saline (1% v/w daily) to ensure adequate hydration until they were sacrificed.

### Immunohistochemistry

After deep anaesthesia with Avertin (250 mg per kg b.w. i.p.), all mice were subjected to *trans*-cardiac perfusion using cold 1x PBS followed by 4% paraformaldehyde. The brains were fixed overnight and dehydrated with 30% sucrose in 1x PBS for 48–72 h before processing. Brain sections (30  $\mu\text{m}$ ) were obtained using a freezing microtome, mounted on the glass





side, and used for both immunohistochemistry and Cresyl Violet staining.<sup>85,86</sup> Nuclei were stained with Santa Cruz mounting media containing DAPI (UltraCruz Aqueous Mounting Medium, SC-24941, Santa Cruz Biotechnology). The visualization of 5BDBD NP (LNP tagged with NR dye) in brain parenchyma in both perilesional cortex of the ipsilateral (stroke side) and cortex of contralateral hemisphere was carried out using a fluorescent microscope.<sup>87,88</sup>

### Cresyl violet staining for infarct volume analysis

To measure infarct volume, eight fixed brain slices were prepared and stained with cresyl violet dye in an alternating pattern, covering the ischemic tissue area. The infarct volumes were quantified by analysing digitalized section images using Sigma Scan Pro software.<sup>89,90</sup> The infarct volumes were presented as a percentage of the contralateral structures with correction for oedema.<sup>22,91</sup> The data analyses were conducted by an investigator who was blinded to the experimental group.

### Statistical analysis

The data are presented as mean  $\pm$  standard deviation (mean  $\pm$  S.D.). Statistical analyses were performed using GraphPad Prism 8 (GraphPad Software, Inc., La Jolla, CA) with a two-way analysis of variance (ANOVA) followed by Tukey's multiple comparisons test to assess the differences between groups with a 95% confidence level ( $p < 0.05$ ). Additionally, unpaired Student's *t*-tests were used for parametric comparisons.

## Conclusions

We have successfully developed liposomal nanocarriers ranging from 50–80 nm in size that encapsulate 5BDBD and Nile red dye. The nanoparticle formulation improved drug solubility, allowing for improved BBB permeability and bio-availability. *In vitro* studies confirmed efficient cellular uptake by human fibroblast cells with no adverse effects on cellular morphology. Additionally, the drug-loaded nanoparticles showed consistent cell viability up to 72 hours. In a mice stroke model, tail vein injection of the nanocarriers demonstrated good biodistribution to the injured brain and significantly reduced infarct volume. The fluorescent nano formulations developed in this study represent a promising platform technology for the delivery of therapeutic agents for stroke.

## Author contributions

Michael R. Arul: data curation, formal analysis, methodology, writing – review & editing. Ibtihal Alahmadi: data curation, formal analysis, methodology, writing – review & editing. Daylin Gamiotea Turro: methodology. ditya Ruikar: writing – review & editing. Sama Abdulmalik: methodology, writing – review & editing. Justin T. Williams: methodology. Basavaraju G. Sanganahalli: formal analysis. Bruce T. Liang: formal analysis. Rajkumar Verma: formal analysis, methodology, supervi-

sion, funding acquisition, writing – review & editing. Sangamesh G. Kumbar: conceptualization, data curation, formal analysis, methodology, project administration, supervision, funding acquisition, writing – review & editing.

## Conflicts of interest

There are no conflicts to declare.

## Acknowledgements

Dr Kumbar acknowledges the funding support by the National Institutes of Biomedical Imaging and Bioengineering of the National Institutes of Health (#R01EB020640, #R56NS122753, and # R01EB030060); the U.S. Army Medical Research Acquisition Activity (USAMRAA), through the CDMRP Peer-Reviewed Medical Research Program under Award No. W81XWH2010321. Dr Verma acknowledges the funding support by the NIH-NINDS grant 1R01NS125405-01A1 and American Heart Association grant 18CDA3411001. The authors also thank Dr Justin Fang for assistance with TEM images.

## References

- 1 S. Lahkar and M. K. Das, in *Multifunctional Theranostic Nanomedicines in Cancer*, Elsevier, 2021, pp. 115–146.
- 2 V. L. Feigin, A. A. Abajobir, K. H. Abate, F. Abd-Allah, A. M. Abdulle, S. F. Abera, G. Y. Abyu, M. B. Ahmed, A. N. Aichour and I. Aichour, *Lancet Neurol.*, 2017, **16**, 877–897.
- 3 A. Achar, R. Myers and C. Ghosh, *Biomedicines*, 2021, **9**, 1834.
- 4 B. A. Witika, M. S. Poka, P. H. Demana, S. K. Matafwali, S. Melamane, S. M. Malungelo Khamanga and P. A. Makoni, *Pharmaceutics*, 2022, **14**, 836.
- 5 M. Tamjid, F. Mahmoudi and A. Abdolmaleki, *Razi Journal of Medical Sciences*, 2022, **28**, 319–336.
- 6 M. Aswar, M. Bhalekar, A. Trimukhe and U. Aswar, *Heliyon*, 2020, **6**, e04482.
- 7 L. Yang, B. M. Conley, S. R. Cerqueira, T. Pongkulapa, S. Wang, J. K. Lee and K. B. Lee, *Adv. Mater.*, 2020, **32**, 2002578.
- 8 K. Goyal, V. Koul, Y. Singh and A. Anand, *Cent. Nerv. Syst. Agents Med. Chem.*, 2014, **14**, 43–59.
- 9 S. Naqvi, A. Panghal and S. Flora, *Front. Neurosci.*, 2020, **14**, 494.
- 10 A. Akbarzadeh, R. Rezaei-Sadabady, S. Davaran, S. W. Joo, N. Zarghami, Y. Hanifehpour, M. Samiei, M. Kouhi and K. Nejati-Koshki, *Nanoscale Res. Lett.*, 2013, **8**, 1–9.
- 11 M. Mohamed, A. S. Abu Lila, T. Shimizu, E. Alaaeldin, A. Hussein, H. A. Sarhan, J. Szebeni and T. Ishida, *Sci. Technol. Adv. Mater.*, 2019, **20**, 710–724.



- 12 F. Zare Kazemabadi, A. Heydarinasab, A. Akbarzadeh and M. Ardjmand, *Artif. Cells, Nanomed., Biotechnol.*, 2019, **47**, 3222–3230.
- 13 K. Gajbhiye, A. Pawar, K. Mahadik and V. Gajbhiye, *Colloids Surf., B*, 2020, **187**, 110770.
- 14 H. Tang, J. Chen, L. Wang, Q. Li, Y. Yang, Z. Lv, H. Bao, Y. Li, X. Luan and Y. Li, *Int. J. Pharm.*, 2020, **573**, 118806.
- 15 Y. Liu, X. Quan, J. Li, J. Huo, X. Li, Z. Zhao, S. Li, J. Wan, J. Li and S. Liu, *Natl. Sci. Rev.*, 2023, **10**, nwac167.
- 16 D. Kuriakose and Z. Xiao, *Int. J. Mol. Sci.*, 2020, **21**, 7609.
- 17 S. Liu, S. R. Levine and H. R. Winn, *J. Exp. Stroke Transl. Med.*, 2010, **3**, 47.
- 18 M. A. Moskowitz, E. H. Lo and C. Iadecola, *Neuron*, 2010, **67**, 181–198.
- 19 P. D. Lyden, F. Bosetti, M. A. Diniz, A. Rogatko, J. I. Koenig, J. Lamb, K. A. Nagarkatti, R. P. Cabeen, D. C. Hess and P. K. Kamat, *Stroke*, 2022, **53**, 1802–1812.
- 20 A. D. Barreto, *Neurotherapeutics*, 2011, **8**, 388–399.
- 21 R. Verma, C. G. Cronin, J. Hudobenko, V. R. Venna, L. D. McCullough and B. T. Liang, *Brain, Behav., Immun.*, 2017, **66**, 302–312.
- 22 P. Srivastava, C. G. Cronin, V. L. Scranton, K. A. Jacobson, B. T. Liang and R. Verma, *Exp. Neurol.*, 2020, **329**, 113308.
- 23 K. L. Nilles, E. I. Williams, R. D. Betterton, T. P. Davis and P. T. Ronaldson, *Int. J. Mol. Sci.*, 2022, **23**, 1898.
- 24 J. J. Mulvihill, E. M. Cunnane, A. M. Ross, J. T. Duskey, G. Tosi and A. M. Grabrucker, *Nanomedicine*, 2020, **15**, 205–214.
- 25 H. Bi, J. Xue, H. Jiang, S. Gao, D. Yang, Y. Fang and K. Shi, *Asian J. Pharm. Sci.*, 2019, **14**, 365–379.
- 26 P. Liu, G. Chen and J. Zhang, *Molecules*, 2022, **27**, 1372.
- 27 M. Çağdaş, A. D. Sezer and S. Bucak, *Application of nanotechnology in drug delivery*, 2014, vol. 1, pp. 1–50.
- 28 F. Rommasi and N. Esfandiari, *Nanoscale Res. Lett.*, 2021, **16**, 1–20.
- 29 V. Dave, A. Gupta, P. Singh, C. Gupta, V. Sadhu and K. R. Reddy, *Nano-Struct. Nano-Objects*, 2019, **18**, 100288.
- 30 P.-W. So, A. Ekonomou, K. Galley, L. Brody, M. Sahuri-Arisoylu, I. Rattray, D. Cash and J. D. Bell, *Int. J. Nanomed.*, 2019, **14**, 1979.
- 31 T. T. Duong, A. Isomäki, U. Paaver, I. Laidmäe, A. Tõnisoo, T. T. H. Yen, K. Kogermann, A. Raal, J. Heinämäki and T.-M.-H. Pham, *Molecules*, 2021, **26**, 2591.
- 32 H. Zhang, *Liposomes: Methods and protocols*, 2017, pp. 17–22.
- 33 M.-M. Song, J. Chen, S.-M. Ye, D.-P. Lu, G.-Y. Zhang, R. Liu and Y.-X. Shen, *Nanomedicine*, 2022, **17**, 741–752.
- 34 H. Ahmad, K. Khandelwal, S. S. Samuel, S. Tripathi, K. Mitra, R. S. Sangwan, R. Shukla and A. K. Dwivedi, *Drug Delivery*, 2016, **23**, 2630–2641.
- 35 Y. Wen, Z. Zhang, Z. Cai, B. Liu, Z. Wu and Y. Liu, *ACS Biomater. Sci. Eng.*, 2022, **8**, 4930–4941.
- 36 J. Wang, Y. Zhang, J. Xia, T. Cai, J. Du, J. Chen, P. Li, Y. Shen, A. Zhang and B. Fu, *J. Am. Heart Assoc.*, 2018, **7**, e007197.
- 37 P. Šimečková, F. Hubatka, J. Kotouček, P. Turánek Knötigová, J. Mašek, J. Slavík, O. Kováč, J. Neča, P. Kulich and D. Hřebík, *Sci. Rep.*, 2020, **10**, 4780.
- 38 L. Shi, J. Zhang, M. Zhao, S. Tang, X. Cheng, W. Zhang, W. Li, X. Liu, H. Peng and Q. Wang, *Nanoscale*, 2021, **13**, 10748–10764.
- 39 J. S. Suk, Q. Xu, N. Kim, J. Hanes and L. M. Ensign, *Adv. Drug Delivery Rev.*, 2016, **99**, 28–51.
- 40 A. Thomas, T. Appidi, A. B. Jogdand, S. Ghar, K. Subramaniam, G. Prabusankar, J. R. Mohanty and A. K. Rengan, *ACS Appl. Polym. Mater.*, 2020, **2**, 1388–1397.
- 41 Y. Zhao, Y. Jiang, W. Lv, Z. Wang, L. Lv, B. Wang, X. Liu, Y. Liu, Q. Hu and W. Sun, *J. Controlled Release*, 2016, **233**, 64–71.
- 42 X. Yang and S. Wu, *Drug Delivery*, 2021, **28**, 2525–2533.
- 43 M. Campos-Martorell, M. Cano-Sarabia, A. Simats, M. Hernández-Guillamon, A. Rosell, D. MasPOCH and J. Montaner, *Int. J. Nanomed.*, 2016, **11**, 3035.
- 44 S. Bernardo-Castro, J. A. Sousa, A. Brás, C. Cecília, B. Rodrigues, L. Almendra, C. Machado, G. Santo, F. Silva and L. Ferreira, *Front. Neurol.*, 2020, **11**, 1605.
- 45 X. Xie, J. Liao, X. Shao, Q. Li and Y. Lin, *Sci. Rep.*, 2017, **7**, 3827.
- 46 A. B. Jindal, *Int. J. Pharm.*, 2017, **532**, 450–465.
- 47 P. Panwar, B. Pandey, P. Lakhera and K. Singh, *Int. J. Nanomed.*, 2010, 101–108.
- 48 Z. Wang, Y. Zhao, Y. Jiang, W. Lv, L. Wu, B. Wang, L. Lv, Q. Xu and H. Xin, *Sci. Rep.*, 2015, **5**, 12651.
- 49 S. Shaker, A. R. Gardouh and M. M. Ghorab, *Res. Pharm. Sci.*, 2017, **12**, 346.
- 50 R. Li, Z. Lin, Q. Zhang, Y. Zhang, Y. Liu, Y. Lyu, X. Li, C. Zhou, G. Wu and N. Ao, *ACS Appl. Mater. Interfaces*, 2020, **12**, 17936–17948.
- 51 S. M. Moghimi, A. Hunter and T. Andresen, *Annu. Rev. Pharmacol. Toxicol.*, 2012, **52**, 481–503.
- 52 P. Decuzzi, B. Godin, T. Tanaka, S.-Y. Lee, C. Chiappini, X. Liu and M. Ferrari, *J. Controlled Release*, 2010, **141**, 320–327.
- 53 E. F. Craparo, M. L. Bondi, G. Pitarresi and G. Cavallaro, *CNS Neurosci. Ther.*, 2011, **17**, 670–677.
- 54 E. Drioli and L. Giorno, *Encyclopedia of membranes*, Springer, 2018.
- 55 T. E. Yalcin, S. Ilbasimis-Tamer, B. Ibisoglu, A. Özdemir, M. Ark and S. Takka, *Pharm. Dev. Technol.*, 2018, **23**, 76–86.
- 56 R. Tremmel, P. Uhl, F. Helm, D. Wupperfeld, M. Sauter, W. Mier, W. Stremmel, G. Hofhaus and G. Fricker, *Int. J. Pharm.*, 2016, **512**, 87–95.
- 57 P. J. Gaillard, C. C. Appeldoorn, J. Rip, R. Dorland, S. M. van der Pol, G. Kooij, H. E. de Vries and A. Reijkerkerk, *J. Controlled Release*, 2012, **164**, 364–369.
- 58 D. Dey, A. Nunes-Alves, R. C. Wade and G. Schreiber, *iScience*, 2022, **25**, 105088.
- 59 F. Alqahtani, P. Belton, A. Ward, K. Asare-Addo and S. Qi, *Int. J. Pharm.*, 2020, **579**, 119172.
- 60 M. Koland, V. Sandeep and N. Charyulu, *J. Young Pharm.*, 2010, **2**, 216–222.
- 61 P. L. Ritger and N. A. Peppas, *J. Controlled Release*, 1987, **5**, 23–36.
- 62 W. I. Higuchi, *J. Pharm. Sci.*, 1967, **56**, 315–324.



- 63 R. W. Korsmeyer, R. Gurny, E. Doelker, P. Buri and N. A. Peppas, *Int. J. Pharm.*, 1983, **15**, 25–35.
- 64 H. N. Alajami, E. A. Fouad, A. E. Ashour, A. Kumar and A. E. B. Yassin, *Pharmaceutics*, 2022, **14**, 131.
- 65 C. Wiegand and U.-C. Hipler, *Skin Pharmacol. Physiol.*, 2009, **22**, 74–82.
- 66 A. L. Nascimento Vieira, M. Franz-Montan, L. F. Cabeça and E. de Paula, *J. Pharm. Pharmacol.*, 2020, **72**, 396–408.
- 67 L. Maione-Silva, E. G. de Castro, T. L. Nascimento, E. R. Cintra, L. C. Moreira, B. A. S. Cintra, M. C. Valadares and E. M. Lima, *Sci. Rep.*, 2019, **9**, 1–14.
- 68 Y.-P. Fang, P.-C. Wu, Y.-H. Tsai and Y.-B. Huang, *J. Liposome Res.*, 2008, **18**, 31–45.
- 69 B. Kloesch, L. Gober, S. Loebisch, B. Vcelar, L. Helson and G. Steiner, *In Vivo*, 2016, **30**, 413–419.
- 70 Z. S. Al-Ahmady, B. R. Dickie, I. Aldred, D. A. Jasim, J. Barrington, M. Haley, E. Lemarchand, G. Coutts, S. Kaur and J. Bates, *Theranostics*, 2022, **12**, 4477.
- 71 M. Arnold, K. Liesirova, A. Broeg-Morvay, J. Meisterernst, M. Schlager, M.-L. Mono, M. El-Koussy, G. Kägi, S. Jung and H. Sarikaya, *PLoS One*, 2016, **11**, e0148424.
- 72 S.-H. Hong, L. Khoutorova, N. G. Bazan and L. Belayev, *Exp. Transl. Stroke Med.*, 2015, **7**, 1–10.
- 73 T. Okada, H. Suzuki, Z. D. Travis and J. H. Zhang, *Curr. Neuropharmacol.*, 2020, **18**, 1187–1212.
- 74 F. Fluri, M. K. Schuhmann and C. Kleinschnitz, *Drug Des., Dev. Ther.*, 2015, 3445–3454.
- 75 K. Dhuri, R. N. Vyas, L. Blumenfeld, R. Verma and R. Bahal, *Cells*, 2021, **10**, 1011.
- 76 N. M. Harris, R. Ritzel, N. S. Mancini, Y. Jiang, X. Yi, D. S. Manickam, W. A. Banks, A. V. Kabanov, L. D. McCullough and R. Verma, *Pharmacol., Biochem. Behav.*, 2016, **150**, 48–56.
- 77 M. R. Arul, C. Zhang, I. Alahmadi, I. L. Moss, Y. K. Banasavadi-Siddegowda, S. Abdulmalik, S. Illien-Junger and S. G. Kumbar, *J. Funct. Biomater.*, 2023, **14**, 52.
- 78 U. Baxa, in *Characterization of Nanoparticles Intended for Drug Delivery*, ed. S. E. McNeil, Springer New York, New York, NY, 2018, pp. 73–88, DOI: [10.1007/978-1-4939-7352-1\\_8](https://doi.org/10.1007/978-1-4939-7352-1_8).
- 79 S. G. Kumbar, K. S. Soppimath and T. M. Aminabhavi, *J. Appl. Polym. Sci.*, 2003, **87**, 1525–1536.
- 80 M. Badran, G. Shazly and M. El-Badry, *Afr. J. Pharm. Pharmacol.*, 2012, **6**, 3018–3026.
- 81 S. Wang, M. Kara and T. Krishnan, *J. Controlled Release*, 1998, **50**, 61–70.
- 82 S. Abdulmalik, D. Ramos, S. Rudraiah, Y. K. Banasavadi-Siddegowda and S. G. Kumbar, *Differentiation*, 2021, **120**, 1–9.
- 83 X. Lu, J. Dong, D. Zheng, X. Li, D. Ding and H. Xu, *Nanomedicine*, 2020, **28**, 102208.
- 84 E. Z. Longa, P. R. Weinstein, S. Carlson and R. Cummins, *Stroke*, 1989, **20**, 84–91.
- 85 H. J. Waldvogel, M. A. Curtis, K. Baer, M. I. Rees and R. L. Faull, *Nat. Protoc.*, 2006, **1**, 2719–2732.
- 86 E. M. Potts, G. Coppotelli and J. M. Ross, *J. Visualized Exp.*, 2020, e61622.
- 87 I. Pirici, T. A. Balsanu, C. Bogdan, C. Margaritescu, T. Divan, V. Vitalie, L. Mogoanta, D. Pirici, R. O. Carare and D. F. Muresanu, *Int. J. Mol. Sci.*, 2017, **19**, 46.
- 88 V. J. Srinivasan, E. T. Mandeville, A. Can, F. Blasi, M. Klimov, A. Daneshmand, J. H. Lee, E. Yu, H. Radhakrishnan and E. H. Lo, *PLoS One*, 2013, **8**, e71478.
- 89 R. Verma, N. M. Harris, B. D. Friedler, J. Crapser, A. R. Patel, V. Venna and L. D. McCullough, *Sci. Rep.*, 2016, **6**, 1–13.
- 90 S. J. Doran, C. Trammel, S. E. Benashaski, V. R. Venna and L. D. McCullough, *Behav. Brain Res.*, 2015, **283**, 154–161.
- 91 R. A. Swanson, M. T. Morton, G. Tsao-Wu, R. A. Savalos, C. Davidson and F. R. Sharp, *J. Cereb. Blood Flow Metab.*, 1990, **10**, 290–293.

